techniques. Moreover, the shortened carbon-carbon (C7-C16) bond length of 1.352 (6) Å indicated a C7-C16 double bond. The ring system N1-C2-C11-C12-C13-C14 is clearly aromatic in nature with an average carbon-carbon bond length of 1.404 (5) Å. The quinoid configuration found for the ring system N4-C5-C6-C7-C8-C3 suggested the possibility of intramolecular electron transfer, inducing carbon-hydrogen bond dissociation in the methyl group at the 4-position in 3,4,7,8-tetramethyl-1,10-phenanthroline.

This led to further investigation of the mechanism involved. A qualitative gas chromatographic examination of the gas above the reaction mixture showed hydrogen and carbon monoxide as well as methane. Subsequently, crystals of another complex (II) were isolated from the same reaction mixture. Mass spectral data for this complex showed a parent molecular ion one mass unit higher than expected for the original 3,4,7,8-tetramethyl-1,10-phenanthroline derivative (415 vs. 414).

These data have led to the proposed mechanism given in Figure 2. Upon reaction, there is an electron transferred from the electron-rich titanium(II) to the aromatic ring, with the greatest electron density of the unpaired electron at C7. This thermally driven electron transfer has been confirmed in bpy(η^5-C_5H_5)$_2$Ti and in phenanthroline complexes which do not contain a methyl group in the 4-position (i.e., C7 or C12 in Figure 1). The electron transfer is also predicted by Fenske-Hall molecular orbital calculations which show a high percent of the carbon p_x character in the highest occupied molecular orbital at this position. The resulting quinoid configuration is also proposed to be an important aspect of flavin electron transfer in biological systems. A bimolecular intermediate through the 4-position, as proposed for the flavin one-electron-transfer process,[9] is probably responsible for subsequent hydrogen radical transfer, leading to the two isolated complexes I and II.

Glass EPR spectra of toluene/benzene (4;1) solutions of I and II at liquid nitrogen temperatures show doublet states for both. These complexes do not account for the triplet-state spectrum observed for the crystallizing solution. Also, the mechanism does not account for the hydrogen and methane gases observed. These gases result from reaction of a methyl or hydrogen radical species upon dissociation of II with the α-hydrogen atoms of the THF or unreacted ligand. The mass spectrum obtained on the gases evolved from the reaction when run in tetrahydrofuran-d_8 shows deuterated methane, suggesting a radical process with the solvent as the primary source of the hydrogen. Compound III, resulting from loss of a methyl radical, could account for the triplet-state spectrum since formally it should be a titanium(II) complex with the possibility of intramolecular electron transfer into a low-lying π^* orbital on the ligand. Loss of a hydrogen radical from II gives the original radical species which can continue through the mechanism. This radical species could also account for the triplet-state spectrum in the crystallizing solution. Ion peaks corresponding to complex III are observed in the mass spectra of I and II.

This intramolecular electron-transfer induced carbon-hydrogen bond dissociation appears to be occurring for all the 4-methyl-substituted 1,10-phenanthrolines but is not observed in the similar 4,4'-dimethyl-2,2'-bipyridyl. Whereas a large contribution for the carbon p_x orbital at the 4-position in the phenanthroline ring was obtained from the molecular orbital calculations, the 4-position in the bipyridyl ring had a smaller electron density. Additional studies are presently being performed to further characterize these systems and other electron-transfer processes leading to alkyl C-H bond dissociation.

Acknowledgments. The support of the National Science Foundation under Grants NSF-DMR-77-23999 and CHE-77-24964 is gratefully acknowledged. The mass spectral data processing equipment was provided by NIH Grants CA 11388 and GM 16864. Thanks are due to D. L. Lichtenberger and P. A. Beak for helpful discussions.

(9) Hemmerich, P. *Adv Chem. Ser.* **1977**, *No. 162*, 312-329.

Supplementary Material Available: The final atomic positional and thermal parameters (Table II), bond distances (Table III), bond angles (Table IV), and a complete listing of structure-factor amplutides (28 pages). Ordering information is given on any current masthead page.

* Present address: Division 5152, Sandia Laboratories, Albuquerque, NM 87185.

D. R. Corbin, W. S. Willis, E. N. Duesler, G. D. Stucky*

Materials Research Laboratory
and School of Chemical Sciences
University of Illinois, Urbana, Illinois 61801
and Sandia Laboratories
Albuquerque, New Mexico 87185

Received March 20, 1980

Substitutive Intramolecular Carbonyl Insertion in a Carbomolybdate Cluster: Formation of a Polycentric, Conformationally Flexible Anion Binding Cavity

Sir:

In the course of a continuing investigation of polyoxomolybdate-carbonyl interactions,[1,2] we have examined the reaction chemistry of the α-dialdehyde glyoxal (OHCCHO). As anticipated,[1] the formylated methylenedioxymolybdate $RCHMo_4O_{15}H^{3-}$, R = OHC, is easily prepared as a tetra-*n*-butylammonium salt from $[(n\text{-}C_4H_9)_4N]_2Mo_2O_7$. Remarkably, however, this anion reacts with certain acids, HX, according to eq 1, resulting in replacement of the OH^- group in the reactant

$$OHCCHMo_4O_{15}H^{3-} + HX \rightarrow HCCHMo_4O_{15}X^{3-} + HOH \quad (1)$$

by an X^- group and insertion of the reactant formylcarbonyl group into a molybdenum-oxygen bond. The product contains a polycentric anion binding site capable of accommodating anions, X^-, having a variety of sizes and shapes. This system offers a rare opportunity for detailed study of (1) the delicate balance between metal-oxygen and carbon-oxygen bond strengths which determines the structure and reactivity of carbomolybdates, (2) mechanistic aspects of polymolybdate-carbonyl interactions, and (3) conformational flexibility in polyoxomolybdate anions.

Reaction of $[(n\text{-}C_4H_9)_4N]_2Mo_2O_7$[3] with an equimolar amount of 70% aqueous $HClO_4$ and excess glyoxal in moist CH_3CN/CH_2Cl_2 followed by addition of ether results in precipitation of a product which analyzes[4] as $[(n\text{-}C_4H_9)_4N]_3OHCCHMo_4O_{15}H$ (**1a**) after crystallization from $CH_2Cl_2/CH_3C_6H_5$. The anion in **1a** is assigned the structure shown in Scheme I[6] on the basis of ^1H NMR and IR data.[4] Addition of compound **1a** in CH_2Cl_2 to an equimolar amount of 49% aqueous HF in CH_3CN followed by precipitation with ether and recrystallization from $CH_2Cl_2/CH_3C_6H_5$ yields block-shaped crystals of $[(n$-

(1) Day, V. W.; Fredrich, M. F.; Klemperer, W. G.; Liu, R. -S. *J. Am. Chem. Soc.* **1979**, *101*, 491-492.

(2) Adams, R. D.; Klemperer, W. G.; Liu, R. -S. *J. Chem. Soc., Chem. Commun.* **1979**, 256-257.

(3) Day, V. W.; Fredrich, M. F.; Klemperer, W. G.; Shum, W. *J. Am. Chem. Soc.* **1977**, *99*, 6146-6148.

(4) Anal. Calcd for $C_{50}H_{111}N_3Mo_4O_{16}$: C, 43.08; H, 8.02; N, 3.01; Mo, 27.53. Found: C, 43.18; H, 8.19; N, 3.15; Mo, 27.47. ^1H NMR[5] (CD_2Cl_2): δ 10.13 (d, 1, $^3J_{HH}$ = 1.3 Hz, O*H*CCHO$_2$), 5.68 (d, 1, $^3J_{HH}$ = 1.3 Hz, OHCC*H*O$_2$). The IR spectrum of **1a** in a Nujol mull shows the identical pattern of absorptions as the spectrum of $[(n\text{-}C_4H_9)_4N]_3CH_2Mo_4O_{15}H^1$ in the 550-950-cm^{-1} Mo-O stretching region and the 3610-3630-cm^{-1} O-H stretching region.

(5) The ^1H NMR spectra of all compounds reported here also display $(n\text{-}C_4H_9)_4N^+$ multiplets centered at ca. δ 3.3, δ 1.5, and δ 1.05.

(6) In Schemes I and II, bonds to molybdenum atoms in the 1.60-1.75-Å range are represented by double lines, bonds to molybdenum atoms whose lengths range between 1.85 and 2.00 Å are represented by single lines, and bonds to molybdenum atoms in the 2.00-2.40-Å range are represented by dotted lines.

0002-7863/80/1502-5971$01.00/0

Scheme I

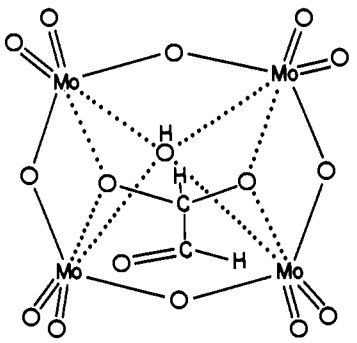

Scheme II

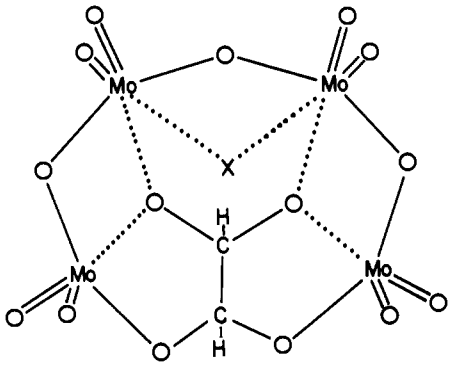

$C_4H_9)_4N]_3HCCHMo_4O_{15}F$[7] (**1b**). The structure of the anion in **1b**, determined by a single-crystal X-ray-diffraction study,[8] is shown in Figure 1a, and selected geometric parameters are given in Table I. The fluorine atom was identified by virtue of the long Mo–F bond lengths and the unique Mo_2–O_F–$Mo_{2'}$ angle; there appears to be no disorder of fluorine and oxygen sites in the anion. Bonding in the **1b** anion is summarized in Scheme II.[6]

Comparison of Schemes I and II reveals the key features of the **1a** to **1b** transformation. Stoichiometrically, the conversion of **1a** to **1b** involves replacement of an OH^- group by an F^- group. The stereochemical consequences of this substitution are considerable; whereas the OH^- group in **1a** is bonded to four 6-coordinate molybdenum atoms, the F^- group in **1b** is bonded to only two metal centers, and the remaining two metals are 5-coordinate. It is presumably the preference of the F^- ion for a doubly bridging bonding mode which permits the observed carbonyl insertion, since the presence of a fourfold bridging ligand like OH^- in **1a** prevents the separation of metal centers which must accompany insertion,

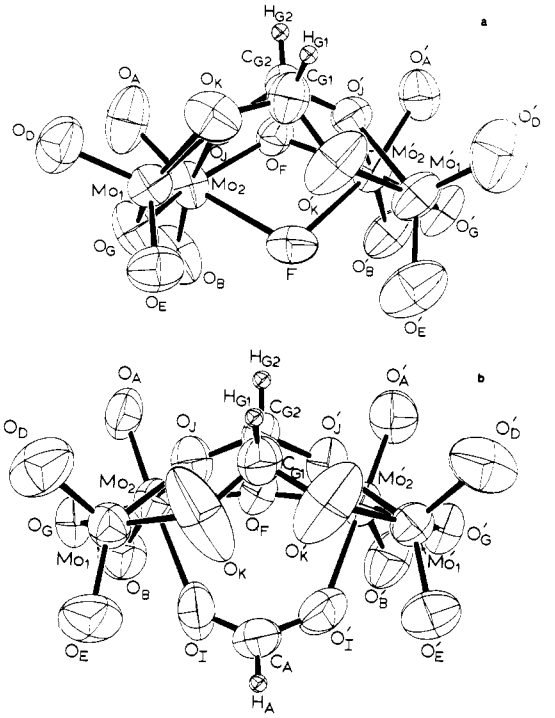

Figure 1. ORTEP drawings of (a) the $HCCHMo_4O_{15}F^{3-}$ anion and (b) the $HCCHMo_4O_{17}CH^{3-}$ anion as observed in solvated single crystals of their $(n\text{-}C_4H_9)_4N^+$ salts. All nonhydrogen atoms are represented by thermal-vibration ellipsoids drawn to encompass 50% of the electron density; the hydrogen atoms are represented by arbitrarily small spheres for purposes of clarity. Molybdenum atoms are labeled with numbers, and oxygen atoms are labeled according to the following scheme: O_A, O_B, O_D, or O_E for terminally bonded oxygens; O_F, O_G, O_I, or O_K for doubly bridging oxygens; and O_J for triply bridging oxygens. The glyoxal carbons are labeled C_{G1} and C_{G2}, the formate carbon in (b) is labeled C_A, and the fluorine atom in (a) is labeled F. Atoms labeled with a prime (′) are related to those without primes by the pseudomirror plane oriented approximately perpendicular to the drawing and ideally containing C_{G1}, C_{G2}, O_F, and F in (a) or C_A in (b).

Table I. Selected Geometric Parameters for the $HCCHMo_4O_{15}X^{3-}$ Anions, X = F (1b) and HCO_2 (1c)

parameter[a]	value[b] 1b	1c
	distances, Å	
Mo_1–$Mo_{1'}$	4.603 (2)	5.143 (2)
Mo_1–Mo_2	3.271 (2, 20)	3.231 (2, 6)
Mo_2–$Mo_{2'}$	3.294 (2)	3.675 (2)
Mo_2–F	2.224 (8, 23)	
Mo_2–O_I		2.297 (13, 41)
Mo_1–F	3.651 (8)	
$Mo_{1'}$–F	3.129 (8)	
Mo_1–O_I		2.962 (16, 37)
C_{G1}–C_{G2}	1.563 (20)	1.525 (20)
	bond angles, deg	
Mo_2–O_F–$Mo_{2'}$	118.7 (4)	149.6 (5)
O_G–Mo_2–O_F	148.9 (4, 5)	149.8 (4, 8)
Mo_1–O_G–Mo_2	117.2 (5, 8)	114.1 (5, 3)
O_K–Mo_1–O_G	146.7 (5, 5)	145.9 (6, 11)
	dihedral angle, deg	
O_K–C_{G2}–C_{G1}/O_J–C_{G2}–C_{G1}	24.7 (···, 16)	6.6 (···, 43)

[a] See Figure 1 for labeling scheme. [b] The first number in parentheses after a value is the root-mean-square estimated standard deviation of an individual datum. If a second number appears in parentheses after a value, the value is the average value of the primed and unprimed parameters, and the number is the deviation of the average from the individual data.

(7) Anal. Calcd for $C_{50}H_{110}N_3Mo_4O_{15}F$: C, 43.01; H, 7.94; N, 3.00; Mo, 27.49; F, 1.36. Found: C, 42.86; H, 7.97; N, 2.98; Mo, 27.30; F, 1.27. ^1H NMR[5] (80 MHz, CD_2Cl_2): δ 6.12 (AB q, 2, $^3J_{AB}$ = 2.7 Hz; $\Delta\nu_{AB}$ = 12.2 Hz, *HCCH*).

(8) Large, well-shaped crystals of the CH_2Cl_2 solvates of **1b** and **1c** were obtained by slow evaporation of $CH_2Cl_2/CH_3C_6H_5$ solutions. Single crystals of **1b** are orthorhombic: space group $Pbcn$-D_{2h}^{14} (No. 60); a = 24.509 (7), b = 24.039 (8), c = 24.050 (6) Å; Z = 8. Those of **1c** are monoclinic: space group $P2_1$-C_2^2 (No. 4); a = 18.400 (3), b = 17.011 (3), c = 12.750 (3) Å; β = 99.77°; Z = 2. Three-dimensional X-ray-diffraction data were collected for the 11 346 independent reflections of **1b** having $2\theta_{Mo\,K\bar{\alpha}} < 48.3°$ and the 5647 independent reflections of **1c** having $2\theta_{Mo\,K\bar{\alpha}} < 45.8°$ on a computer-controlled four-circle Syntex P_1 autodiffractometer by using graphite-monochromated Mo K$\bar{\alpha}$ radiation and full (1° wide) ω scans. For each compound, the four molybdenum atoms of the totally general position asymmetric unit were located by using direct methods (MULTAN); the remaining anionic and cationic nonhydrogen atoms and the anionic hydrogen atoms were located by standard difference Fourier techniques. The resulting structural parameters for **1b** have been refined to convergence [R (unweighted, based on F) = 0.062 for 5116 independent reflections having $2\theta_{Mo\,K\bar{\alpha}} < 43°$ (the equivalent of 0.50 limiting Cu K$\bar{\alpha}$ spheres) and $I > 3\sigma(I)$] by using unit-weighted full-matrix least-squares techniques with anisotropic thermal parameters for all anionic and solvent nonhydrogen atoms and isotropic thermal parameters for the cationic nonhydrogen atoms and anionic hydrogen atoms. The parameters for **1c** have been refined to convergence in a similar fashion [R (unweighted, based on F) = 0.055 for 4704 independent reflections having $2\theta_{Mo\,K\bar{\alpha}} < 45.8°$ (the equivalent of 0.60 limiting Cu K$\bar{\alpha}$ spheres) and $I > 3\sigma(I)$]. Refinement of both compounds is continuing with those reflections having $I > 3\sigma(I)$ for the more complete data sets and models, which include anisotropic thermal parameters for all nonhydrogen atoms and isotropic thermal parameters for locatable hydrogen atoms.

As might be expected from the structural relationship between **1a** and **1b**, labeling experiments provide support for an intramolecular insertion mechanism. We have prepared $[(n\text{-}C_4H_9)_4N]_3CH_3COCHMo_4O_{15}H$[9] (**2a**) by following the procedure outlined above for the preparation of compound **1a** but replacing glyoxal with methylglyoxal (CH_3COCHO). Compound **2a**, structurally related to **1a** by replacement of its aldehyde proton with a methyl group, reacts with HF in an analogous fashion to yield $[(n\text{-}C_4H_9)_4N]_3CH_3CCHMo_4O_{15}F$ (**2b**).[10] The ^1H NMR spectrum of pure compound **2b**, crystallized by slow (2 days) evaporation from $(CH_3)_2CO/CH_3C_6H_5$, in CD_2Cl_2, displays two acetal proton resonances at δ 6.05 and δ 5.83 having relative intensities of 3:2. These resonances presumably arise from the two isomers of **2b**, where the methyl group is bound to either the central or the peripheral acetal carbon (see Scheme II). The ^1H NMR spectrum of crude **2b** in CD_2Cl_2 displays only one acetal resonance at δ 6.05. If the NMR solution is allowed to stand, however, the second δ 5.83 acetal resonance appears and slowly grows in intensity as the δ 6.05 resonance loses intensity until a final intensity ratio of 3;2 is observed after 20–40 h. These observations show that the **2a** to **2b** transformation is regiospecific but that the product rearranges in solution. If one assumes that the methyl group in the kinetically favored product is bound to the peripheral carbon atom (see Scheme II), the NMR data support an insertion mechanism.

The conformational flexibility of the F^- binding site in compounds **1b** and **2b** is evident from the anion structure of $[(n\text{-}C_4H_9)_4N]_3HCCHMo_4O_{17}CH$ (**1c**),[11] determined by an X-ray-diffraction study,[8] shown in Figure 1b. Compound **1c** is prepared according to eq 1, HX = HCO_2H, utilizing conditions similar to those employed for the synthesis of compound **1b** (see above). Comparison of Figure 1a,b and data given in Table I shows how the geometry of the $HCCHMo_4O_{15}^{2-}$ unit is adjusted to accommodate either the F^- anion or the larger HCO_2^- ion. Expansion of the $Mo_2\text{–}O_F\text{–}Mo_{2'}$ angle increases the $Mo_2\text{–}Mo_{2'}$ separation. As this Mo–Mo distance changes, however, the remainder of the anion geometry must be adjusted. The necessary flexibility is provided by rotation about the $C_{G1}\text{–}C_{G2}$ bond which varies the $Mo_1\text{–}Mo_{1'}$ distance and, together with expansion or contraction of the $Mo_2\text{–}O_F\text{–}Mo_{2'}$ angle, determines the size of the anion binding cavity.

Acknowledgments. W,G,K. acknowledges the National Science Foundation and the donors of the Petroleum Research Fund, administered by the American Chemical Society, for support of this research.

Supplementary Material Available: Tables of atomic positional and thermal parameters for compounds **1b** and **1c** (8 pages). Ordering information is given on any current masthead page.

(9) Anal. Calcd for $C_{51}H_{113}N_3Mo_4O_{16}$: C, 43.50; H, 8.09; N, 2.98; Mo, 27.25. Found: C, 43.58; H, 8.30; N, 3.01; Mo, 27.49. ^1H NMR[5] (CD_2Cl_2): δ 5.77 (s, 1, CH_3COCH), 2.53 (s, 3, CH_3COCH). The IR spectra of **2a** and **1a** in Nujol mulls show the same pattern of absorptions in the 550–950-cm^{-1} Mo–O and the 3610–3630-cm^{-1} O–H stretching regions.

(10) Anal. Calcd for $C_{51}H_{112}N_3Mo_4O_{15}F$: C, 43.44; H, 8.01; N, 2.98; Mo, 27.21; F, 1.35. Found: C, 43.31; H, 8.08; N, 2.94; Mo, 27.10; F, 1.39.

(11) Anal. Calcd for $C_{51}H_{111}N_3Mo_4O_{17}$: C, 43.07; H, 7.87; N, 2.95; Mo, 26.98. Found: C, 43.18; H, 7.85; N, 3.12; Mo, 27.09. ^1H NMR[5] (80 MHz, CD_2Cl_2): δ 8.53 (s, 1, HCO_2), 6.05 (AB q, 2, $^3J_{AB}$ = 3.2 Hz, $\Delta\nu_{AB}$ = 7.9 Hz, $HCCH$).

(12) Camille and Henry Dreyfus Teacher-Scholar.

V. W. Day,*[12] M. R. Thompson
Department of Chemistry, University of Nebraska
Lincoln, Nebraska 68588

C. S. Day
Crystalytics Company
Lincoln, Nebraska 68501

W. G. Klemperer,*[12] R.-S. Liu
Department of Chemistry, Columbia University
New York, New York 10027
Received March 31, 1980

A Novel β-Ketophosphonate 1,4-Dianion. Tin/Lithium Exchange

Sir:

In recent years, carbon–carbon bond formation by means of regiospecific reaction of dianions and dianion analogues has become an increasingly important synthetic tool.[1] Monoanions derived from β-ketophosphonate esters have been extremely useful in the synthesis of certain olefins from aldehydes and ketones.[2] Elegant uses of β-ketophosphonate 1,3-dianions (**1**) have been

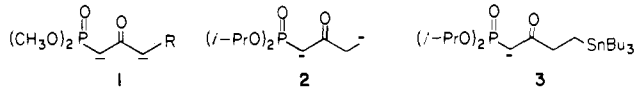

1 2 3

reported.[3] I report here the generation of β-ketophosphonate 1,4-dianion **2** via the tin/lithium exchange of the monoanion (**3**) derived from diisopropyl 4-tri-*n*-butylstannyl-2-oxobutylphosphonate (**4**). The generation of **2** provides a method of

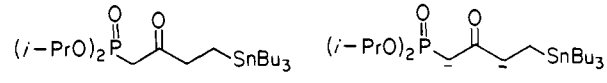

4 5

functionalizing the δ carbon of a β-ketophosphonate ester and shows for the first time that it is possible to generate a thermodynamically less stable 1,4-dicarbanion via tin/lithium transmetalation even when an alternative proton abstraction to produce a more stable 1,3-dicarbanion (**5**) is available.[4–6]

The generation of organolithium reagents from organotin compounds is a very well-known and widely used reaction.[7] These tin/lithium exchange reactions appear to be equilibrium processes, and they are usually successful only when the organolithium reagent to be generated is stabilized either by unsaturation or by a heteroatom.[8–10] For example, Seyferth and Weiner[8] were unable to prepare the corresponding lithio compound from (3-butenyl)tri-*n*-butyltin. Presence of a carbanionic center in the molecule also retards the tin/lithium transmetalation reactions.[11,12] The success of tin/lithium exchange in the case of **3** is possibly due

(1) (a) For a review on dianions of β-dicarbonyl compounds, see: Harris, T. M.; Harris, C. M. *Org. React. (N.Y.)* **1969**, *17*, 155. (b) For a review on dianions and polyanions, see: Kaiser, E. M.; Petty, J. D.; Knutson, P. L. A. *Synthesis* **1977**, 509–550. (c) Hubbard, J. S.; Harris, T. M. *J. Am. Chem. Soc.* **1980**, *102*, 2110. (d) Trimitsis, G. B.; Hinkley, J. M.; Ten Brink, R.; Poli, M.; Gustafson, G.; Erdman, J.; Rop, D. *Ibid.* **1977**, *99*, 4838. (e) Weiler, L. *Ibid.* **1970**, *92*, 6702. (f) Bays, J. P. *J. Org. Chem.* **1978**, *43*, 38. (g) Cooke, M. P., Jr. *Ibid.* **1973**, *38*, 4062.

(2) (a) For a review, see: Boutagy, J.; Thomas, R. *Chem. Rev.* **1974**, *74*, 87–99. (b) For some recent uses, see: Meyers, A. I.; Smith, R. K. *Tetrahedron Lett.* **1979**, 2749. Stork, G.; Nakamura, E. *J. Org. Chem.* **1979**, *44*, 4010. Nicolaou, K. C.; Seitz, S. P.; Pavia, M. R.; Petasis, N. A. *Ibid.* **1979**, *44*, 4011.

(3) (a) Grieco, P. A.; Pogonowski, C. S. *J. Am. Chem. Soc.* **1973**, *95*, 3071. (b) *Synthesis* **1973**, 425. (c) Grieco, P. A.; Finkellor, R. S. *J. Org. Chem.* **1973**, *38*, 2909.

(4) Generation of the 1,4-dianion $LiCH_2CH_2CO_2Li$ from $BrCH_2CH_2CO_2Li$ and lithium naphthalenide via halogen/metal exchange has been reported; see: Caine, D.; Frobese, A. S. *Tetrahedron Lett.* **1978**, 883.

(5) It is assumed that the presence of tri-*n*-butyltin in the molecule did not greatly affect the stability of such a dianion. There is evidence in the literature to suggest that the presence of tri-*n*-butyltin in such a position of a carbanion does not change the behavior of the carbanion. See: Teratake, S.; Morikawa, S. I. *Chem. Lett.* **1975**, 1333. Still, W. C. *J. Am. Chem. Soc.* **1977**, *99*, 4836.

(6) Seebach, D.; Geiss, K. H. *J. Organomet. Chem. Libr.* **1976**, *1*, 5. In this example, Sn/Li exchange is faster than epoxide opening by BuLi at –100 °C.

(7) For a review, see ref 6, pp 188–190.

(8) Seyferth, D.; Weiner, M. A. *J. Am. Chem. Soc.* **1962**, *84*, 361.

(9) Still, W. C. *J. Am. Chem. Soc.* **1978**, *100*, 1481.

(10) Piers, E.; Morton, H. E. *J. Org. Chem.* **1979**, *44*, 3437.

(11) Seyferth, D.; Vick, S. C. *J. Organomet. Chem.* **1978**, *144*, 1.

(12) One example of a successful tin/lithium exchange of a lithio compound, $LiOCH_2SnBu_3$, has been reported: Seebach, D.; Meyer, N. *Angew. Chem., Int. Ed. Engl.* **1976**, *15*, 438. This was accomplished under forcing conditions (petroleum ether, room temperature, 6 h) in moderate yield.

0002-7863/80/1502-5973$01.00/0